energies

Article

A Comprehensive Framework for Enhancing Distribution System Resilience Under Heatwave Conditions

Luigi Calcara [1], Adriano Casu [2,*], Fabrizio Pilo [2], Giuditta Pisano [2], Maurizio Pollino [3], Massimo Pompili [1] and Maria Luisa Villani [3]

[1] Department of Electrical and Energetic Engineering, University of Rome "La Sapienza", Via Eudossiana 18, 00184 Rome, Italy; luigi.calcara@uniroma1.it (L.C.); massimo.pompili@uniroma1.it (M.P.)
[2] Department of Electrical and Electronic Engineering, University of Cagliari, Via Marengo 2, 09123 Cagliari, Italy; fabrizio.pilo@unica.it (F.P.); giuditta.pisano@unica.it (G.P.)
[3] Italian National Agency for New Technologies, Energy and Sustainable Economic Development (ENEA), Via Anguillarese 301, 00123 Rome, Italy; maurizio.pollino@enea.it (M.P.); marialuisa.villani@enea.it (M.L.V.)
* Correspondence: adriano.casu@unica.it

Abstract

This paper presents a lightweight method for assessing the resilience of power distribution systems that integrates climate and infrastructure data through impact chains and a probabilistic approach, while minimizing data integration and implementation complexity. The method is demonstrated for heatwave hazards by combining network characteristics, failure probabilities of heat-sensitive components (e.g., medium-voltage cable joints), and location-specific climate projections to generate spatial maps of failure risk and network resilience. These maps support the identification and prioritization of critical components requiring intervention. Critical segments are then further analyzed using probabilistic resilience metrics to compare alternative adaptation strategies. Overall, this work contributes a practically applicable, low-complexity methodology for identifying the weakest portions of distribution networks, along with a more in-depth probabilistic approach for assessing their climate resilience. The comprehensive framework is illustrated through a case study of a representative portion of the Italian electricity distribution system in the urban area of Rome. It is implemented in a test environment that reflects realistic distribution network data structures and automatically integrates climate data from established online repositories.

Keywords: heatwaves; resilience; electrical distribution system; knowledge graph; impact chains; risk index

Academic Editor: Pavlos S. Georgilakis

Received: 11 March 2026
Revised: 15 April 2026
Accepted: 16 April 2026
Published: 17 April 2026

1. Introduction

Climate change is driving an increase in the frequency and intensity of extreme events, to which critical infrastructure, including power systems, is particularly vulnerable [1]. Factors such as aging infrastructure, evolving operational conditions for electrical utilities, and shifting network usage patterns driven by decarbonization goals all heighten the sensitivity of these systems to high-impact, low-frequency (HILF) events [2]. A key driver is the steady rise in global temperatures. Although Representative Concentration Pathways (RCPs) are scenarios aimed at limiting warming, projections indicate that heatwaves will increase in frequency, intensity, and duration relative to historical events [3]. Heatwaves place substantial stress on power systems, particularly on distribution systems (i.e., medium-

and low-voltage networks, MV and LV), leading to equipment failures, component overheating, and voltage fluctuations. This issue poses several research challenges, requiring updates to both network analysis methods and supporting tools to adequately account for system-level considerations, encompassing the network itself and the interacting natural and social environments.

From an analytical perspective, unlike other natural hazards such as earthquakes, where fragility curves like those implemented in HAZUS [4] are well-established, the analysis methods for power networks under climate change-related phenomena still face significant challenges. Indeed, these phenomena—particularly heatwaves—which are inherently dynamic and location-specific, lack widely accepted and validated systemic models to assess their impacts on networks. Consequently, supporting analysis technology must not only be updated functionally and expanded toward a systemic perspective of the methods, but also remain flexible, easy to adopt, and adaptable to model updates [5].

In [6,7], an efficient methodology for identifying relevant multiple contingencies to perform resilience-oriented long-term planning was proposed. The methodology relies on creating a correlation matrix that links contingencies derived from historical data to network vulnerable components. The approach's validity is demonstrated across a large portion of the transmission grid. In this case, the covered region is vast, but the number of vulnerable components (thus the dimension of the correlation matrix) remains small. The dimensions grow significantly when analyzing large-scale distribution networks, leading to possible computational issues and, more importantly, data availability issues. When available, network data for power distribution systems is often aggregated (especially in low-voltage networks), which undermines the validity of these approaches.

Moving to the distribution level, a recent review highlighted the urgent need to appropriately model the complex operational decision-making problems in large-scale power distribution systems [8]. This issue is not sufficiently addressed in the literature. While a consistent effort has been made to develop Geographic Information System (GIS)-based approaches for resilience assessment, as in [9–11], the considered scale is often limited and insufficient to incorporate resilience into distribution system development plans.

This paper moves in this direction by proposing a lightweight, large-scale resilience analysis approach for distribution networks against heatwaves. The approach is based on impact chains, whose proven effectiveness is well-documented in the climate and resilience analysis literature [12,13]. It is supported by a flexible technological method for integrating and processing climate, infrastructure, and territorial data [5]. Planning resilient distribution systems against heatwaves first requires identifying indicators related to the specific hazard event, network characteristics (particularly those concerning underground cables, which are among the most vulnerable network components to heatwaves), and social factors. These indicators are then used to probabilistically quantify risk and evaluate the effectiveness of resilience enhancement strategies that can be implemented.

Recent studies [14,15] applied Machine Learning (ML) techniques to support fault prediction in distribution grids under heatwave conditions, leveraging fault time series provided by the network operator. More generally, machine learning approaches use historical datasets (infrastructure-specific) to train predictive models. However, these datasets reflect past climatic conditions and infrastructure states, which may not adequately represent future hazard scenarios under climate change and evolving infrastructure conditions. In contrast, the proposed approach is scenario-driven and simulation-based, enabling the analysis of hypothetical conditions and alternative assumptions that may not be captured in historical datasets.

The methodology is implemented through a tool-supported process that starts with the acquisition of climate data and the automatic calculation of the indicators. Through

interaction with a GIS for data contextualization, and by combining hazard indicators, network characteristics, failure probabilities of electrical grid components most affected by heatwaves, and impact, network risk or resilience maps are generated. This kind of representation is particularly effective when used as decision support and is often exploited in the climate and resilience analysis literature, as in [7]. The approach exploits knowledge graph technology, linking diverse data, information, and models to an application ontology focused on the resilience of electricity systems, to support the integrated processing and visualization of relevant information for decision-making [16]. The network portions identified as critical in the maps are further analyzed using a probabilistic approach, with resilience metrics computed to compare alternative enhancement strategies. The overall process is illustrated through a case study that places a representative portion of the Italian electricity distribution system supplied by a primary substation in the urban area of Rome.

A preliminary version of this work, focusing on the methodological framework, was presented in [17]. This extension offers a more comprehensive integration of the methodology with the developed tools, as detailed in the new section dedicated to the case study. Specifically, it illustrates the setup of a test-bed analysis environment that leverages open data and provides interoperable interfaces with existing data sources, including climate repositories and network description models. Furthermore, using a Monte Carlo simulation approach and performing power flow calculations, suitable resilience metrics are assessed to evaluate possible solutions to improve network resilience. The resilience assessment results are reported and discussed.

The proposed resilience assessment test-bed is platform-independent and generalizable, enabling diverse user groups, such as municipal stakeholders or private citizens, to contribute to strategy formulation while protecting sensitive data and ensuring the integrity of operators' proprietary information systems. It is important to note that detailed, high-resolution datasets on component failures in distribution networks are typically not publicly available, limiting the ability to validate against real outage data directly. In this context, the objective of this work is primarily methodological: to develop and demonstrate a framework for integrating climate-related stressors into resilience assessments. Therefore, the use of simulated scenarios is a necessary approach for systematically analyzing system behavior and evaluating the potential impact of extreme weather conditions under controlled, reproducible conditions. This work proposes a framework applicable to any distribution system serving a specific geographical area; it is data-driven, so the confidence in the results depends on the reliability of the inputs, which are relevant to climate projections and distribution network assets. The main interest is to highlight that the framework can differentiate risky areas from safe ones, starting from hypotheses based on other studies (e.g., those that estimate the probability of occurrence of an extreme event), and can evaluate the resilience level achieved when certain enhancing actions are implemented. While validation with field data would be desirable, the proposed methodology is adaptable and can be applied directly when such datasets become available. Furthermore, in this paper, the extreme event under consideration is the heatwave, but the framework can be applied to any severe climate hazard.

This contribution is part of the activities of the project "Network 4 Energy Sustainable Transition—NEST", funded under the National Recovery and Resilience Plan (NRRP).

2. Resilience Against Heatwaves: Methods and Tools

This section describes the methods and tools adopted in this work. First, heatwaves are introduced as the reference climate hazard, and the indicator used to characterize heat-stress conditions is described. It is worth noting that, although the correlation between high temperatures and power distribution system failures is demonstrated, the relationship

is not straightforward. Second, the impact-chains approach is used for identifying the most critical portion of a distribution system/network under heatwave conditions, detailing the integration of climate indicators, component vulnerability, and network characteristics. Furthermore, based on the results of such a lightweight calculation, a more in-depth analysis can be applied to the weakest areas to support decision-makers who must drive climate resilience investments. Finally, the tools supporting the method's implementation are outlined, with emphasis on data integration, the analysis workflow, and the computation of the resilience metric.

2.1. Heatwave Impacts on Electrical Grids

Heatwaves, defined as prolonged periods of anomalously high temperatures often accompanied by drought, are increasingly recognized as a critical stressor for power distribution systems. Their impacts are not limited to rising electricity demand but extend to the physical degradation of MV and LV electrical infrastructures. As highlighted in [18,19] and in continuity reports published by ARERA [20], heatwaves significantly alter failure probabilities of distribution assets, amplify service interruptions, and pose systemic risks to network resilience.

The resilience of MV grids depends heavily on the reliability of underground cable lines, particularly their joints, which are the most fragile components. During summer periods, extreme heat combined with limited precipitation intensifies stress on these elements due to reduced heat dissipation, potentially leading to overheating, partial discharge activity, and eventual failure.

A well-documented correlation exists between heatwaves and the frequency of failures in MV underground joints. Both elevated ambient temperatures and soil dryness undermine the dissipation of heat generated by Joule losses. Under these conditions, failures have been observed to increase by 4–6 times the average seasonal rate [19]. However, a standardized relationship between heatwave occurrence and the number of faults has not been established. It can be derived only from historical and experimental data available in Distribution System Operators (DSO) rooms.

One of the most influential parameters driving failure rates is the variation in soil thermal resistivity. In summer, the lack of rainfall leads to soil drying, increasing thermal resistance and impairing the surrounding medium's capacity to dissipate heat from buried cables. This effect is particularly pronounced during extended heatwaves, when ground temperatures remain elevated for prolonged periods. The resulting thermal stress accelerates the degradation of insulation materials within joints, undermining dielectric strength and facilitating the onset of partial discharges.

Insulation deterioration in MV cable joints is a progressive process exacerbated by repeated thermal stress. Prolonged exposure to elevated temperatures weakens polymeric materials, reducing their capacity to withstand electrical stress. Furthermore, the manual nature of joint assembly introduces micro-defects and vacuoles that, though often unavoidable, act as focal points for stress concentration. Under heatwave conditions, these imperfections accelerate the onset of partial discharges, increasing the probability of failure.

Failure trends consistently reflect a seasonal dependence tied to climatic stressors.

The bar graph in Figure 1 illustrates the normalized trend of failures of medium-voltage underground cable joints over a representative year of the last decade. The failure rate remains low and stable from January to April, then rises sharply in May, reaching its peak in June and July (up to 4–6 times the seasonal average). After July, the rate tends to decrease in August, then stabilizes at relatively low levels from September through December. This seasonal cycle reinforces the established link between cable joint failures and prolonged heatwaves.

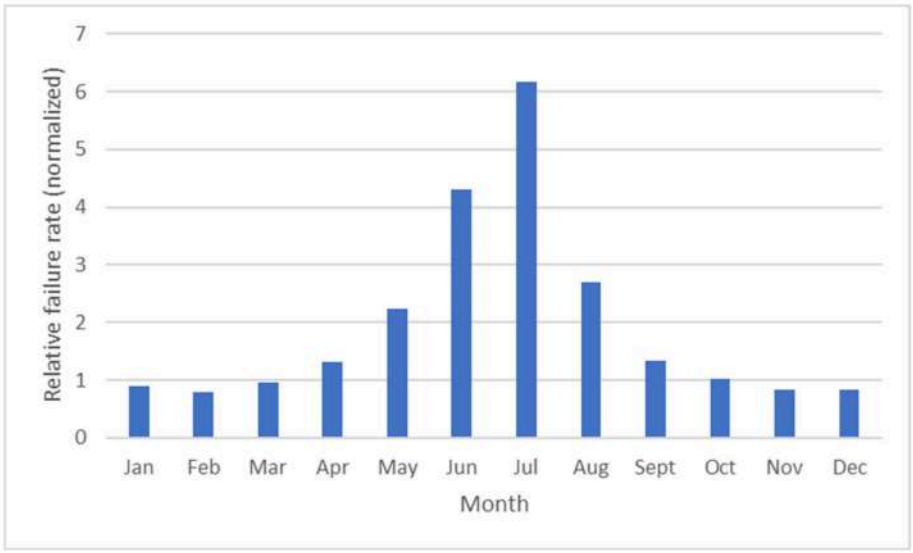

Figure 1. Normalized trend of failures of medium-voltage underground cable joints over a representative year of the last decade.

DSOs currently use several indicators to monitor the occurrence of grid faults associated with consecutive hot days, typically characterized by high temperatures and a lack of rainfall.

These indicators incorporate thresholds, such as minimum, mean, or maximum daily temperatures over a specified period, that serve as reference criteria for defining heatwave days. Among the thresholds adopted by major Italian electrical distribution operators, and formalized in the formula reported below, is a critical temperature of approximately 33 °C. Historical analyses identified this threshold as the point beyond which the incidence of faults in medium-voltage underground cables significantly exceeded the average annual fault rate. Given the ongoing progression of climate change, a re-evaluation of such thresholds may be warranted to ensure their continued relevance and robustness.

The formula used to calculate heatwave days, officially recognized by ARERA (Italian Regulatory Authority for Energy, Networks and Environment), is the following (1).

$$HWI_{heatwave} = \sum_{i=1}^{7} \left(n_{TMAXi} + n_{pi} - \frac{p_i}{10} \right), \quad (1)$$

where

- $HWI_{heatwave}$ is the heatwave index for a specific moving window (likely a week, since the summation runs from 1 to 7).
- n_{TMAXi} is the number of days where the maximum temperature exceeds the threshold value equal to 33 °C;
- n_{pi} is the number of days without rain;
- $\frac{p_i}{10}$ is the penalty or adjustment factor that reduces the influence of the high temperatures over time and is proportional to the centimeters of daily precipitation.

Equation (1) uses a temperature threshold and a precipitation-related correction factor that should not be regarded as universally applicable parameters, but rather as context-dependent quantities adopted here for the specific case study. For applications in regions different from the Mediterranean area, hazard characterization can be recalibrated by adopting locally relevant thresholds and climate descriptors. For example, the fixed temperature threshold may be replaced by percentile-based thresholds derived from long-term local climatology, or by critical temperature values identified from historical correlations between weather conditions and component failures. Similarly, the precipitation term

may be reformulated, omitted, or integrated with additional variables, such as soil moisture or the persistence of high night-time temperatures, depending on the dominant local heat-stress mechanisms. In this sense, the proposed framework is general, whereas the specific heatwave index formulation must be adapted to the climatic and operational context under study.

2.2. Resilience Assessment

Embedding resilience enhancement into distribution system planning is no longer optional. This requires extending decision support tools with resilience-oriented analysis methods while strengthening energy security, advancing decarbonization goals, and protecting vulnerable communities. However, several challenges arise from this need. First, resilience must be measured, possibly with tools easy to use even for policy makers unfamiliar with power systems, that require high-level information about the infrastructure serving the territories they manage.

Proposals for power system resilience metrics are presented in various papers [21–25]. Recently, systems operators introduced four attributes and determinants for defining a resilient system [26]:

- Robustness, i.e., "the ability of systems, system elements, and other units of analysis to withstand disaster forces without significant degradation or loss of performance".
- Redundancy, i.e., "the extent to which systems, system elements, or other units are substitutable, that is, capable of satisfying functional requirements, if significant degradation or loss of functionality occurs".
- Resourcefulness, i.e., "the ability to diagnose and prioritize problems and to initiate solutions by identifying and mobilizing material, monetary, informational, technological, and human resources".
- Rapidity, i.e., "the capacity to restore functionality in a timely way, containing losses and avoiding disruptions".

A recent work proposed adapting the impact chains approach to the power systems [27]. A generic impact chain links to the expected risk, hazard, exposure, and vulnerability, which is distinguished by sensitivity and adaptation (Figure 2). This approach perfectly fits with the four determinants that define a resilient power system, because it considers, at the same time, the impact of the severe weather event (the hazard) on the system quality, which increases with the exposed assets and with the sensitivity of its users (it concerns the robustness of the system), and the evolution of the recovery, that is a measure of the adaptation capability of the system. Recovery includes the time needed to identify the faulted area of the network, the time the DSO spends organizing the restoration process (reflecting its resourcefulness), and, finally, the recovery time itself (reflecting its rapidity, while also involving aspects of resourcefulness and redundancy).

Figure 2. Generic impact chain.

Each component of the chain is represented by suitable indicators relevant to the specific extreme event considered, as these vary depending on the type of hazard and the network's capacity to withstand it. Thus, one part of the distribution system may tolerate, for instance, wind or snow storms well [28], whereas another may fail under heatwaves.

Regarding heatwaves, as mentioned, the most vulnerable grid elements are MV cable joints, so urban networks are expected to be less resilient than rural grids. Urban networks typically have many secondary substations, each supplying high demand to numerous customers, interconnected by short underground cables with several joints. In contrast, rural grids predominantly consist of long overhead lines with low load demand density.

In [26], the European Distribution System Operators (E.DSO) list a significant number of indicators, classified by resilience feature, event phase, and weather case. Among these many indicators, Table 1 reports the ones suitable for heatwaves used in this paper.

Table 1. Indicators of impact chains elements for heatwaves.

Hazard	***Heatwaves Index $HWI_{heatwave}$ (as defined in (1))***
Exposure	Underground cable length Number of joints Joint average age
Sensitivity	Number of LV customers Number of MV customers Number of prosumers Number of premium customers
Adaptation	Distributed generation or storage installed power Trunk nodes

Regarding the exposure indicators, which include the MV cable joints as the only vulnerable components, it is worth noting that distribution systems contain several component types that may be vulnerable to heatwaves, such as transformers and protection devices. In this paper, MV cable joints are prioritized because they represent a particularly relevant heat-sensitive component in the considered urban underground distribution network and because previous studies, as well as the operational context of the case study, indicate that these elements are among the most exposed to thermally induced failures during extreme summer conditions. However, the framework is designed to be extensible to other component types, including transformers, switchgears, etc. Their inclusion would require defining additional component-specific hazard–response relationships and fragility assumptions, which may change the resulting resilience rankings, depending on the network topology and local asset mix.

Once defined, the indicators (as the ones in Table 1) must be calculated for the understudy portion of the network/territory and combined with a simple weighted mean calculation, as in (2), where I_g is the value of the generic chain index (i.e., it can be the exposure index I_E, the sensitivity index I_S, the adaptation index I_A or the final risk index I_R); $I_{g,i}$ is the value of the g,i-th normalized specific indicator of the generic chain element; $w_{g,i}$ is the weight assigned to the g,i-th specific indicator; and n_g is the generic number of indicators.

$$I_g = \frac{\sum_{i=1}^{n_g} I_{g,i} \cdot w_{g,i}}{\sum_{i=1}^{n_g} w_{g,i}} \quad (2)$$

The specific indicators, and thus the risk indicator, are calculated for each small portion on which the considered territory is subdivided. It is worth noting that the resulting risk indexes provide only high-level information and do not require power flow calculations, even if for evaluating the sensitivity (e.g., the number of customers interrupted downstream

a faulted branch) and the adaptation (e.g., the number of trunk nodes that can be part of an alternative path for de-energized portions of the networks) indicators it is needed to know the topology of the network. Once the relevant components of the supply chain are defined for a specific portion of the network or territory, such an approach is easy to implement. The unnecessary power flow calculations make this approach suitable for large-scale applications without burdening the analysis. The use of a weighted-average aggregation may appear to be a simplification of complex system interactions. However, this choice is motivated by the need to ensure computational efficiency and transparency of the methodology, which are key requirements for supporting decision-making processes. In particular, at this stage, the proposed approach aims to provide a first-level identification of critical assets, making it suitable for policymakers and planners who require scalable, interpretable tools. Moreover, the careful selection and calibration of the weighting factors allow for preserving the relative importance of different system components, thereby mitigating the risk of losing relevant interaction effects during aggregation. Therefore, the adopted aggregation represents a trade-off between model complexity and practical applicability, without compromising the validity of the main insights.

However, because network investments can be high, more rigorous studies should be conducted to identify the most effective planning options to enhance the resilience of the weakest portion of the network. For this reason, this paper proposes an in-depth analysis of the network portions that proved critical based on high-level indexes derived from the impact chains. For such analysis, a resilience metric is proposed, able to be incorporated alongside conventional reliability measures (e.g., indicators such as Customer Minutes Lost (CMLs) or System Average Interruption Duration Index (SAIDI) and Customer Interruptions (CIs) or System Average Interruption Frequency Index (SAIFI)), system vulnerabilities associated with climate-driven HILF events, and the possibility that the impact of the event involves more than one network component (N-k approach).

The specific resilience metric used in the paper is the area of the resilience trapezoid, which is an extension of the resilience triangle (Figure 3). Its assessment implies in-depth analyses of the network and power flow calculations.

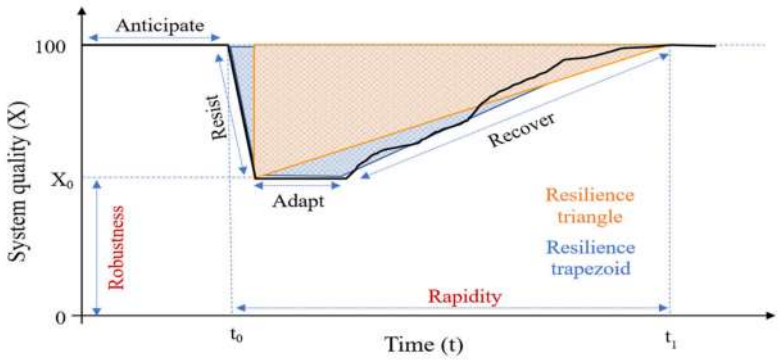

Figure 3. Examples of metrics: resilience triangle and resilience trapezoid areas.

Such a metric identifies how low the system quality drops and how promptly the system operator restores the service. The depth X_0 of the geometric figure measures the impact on the system quality drop, or, in other words, the network's robustness, and its gradient reflects how quickly the hazard evolves. After the acute phase of the disaster, the adaptation period (i.e., the time the DSO takes to organize recovery, which depends on the DSO's resourcefulness) and the recovery period (i.e., the time required to restore service to all customers) begin. Reducing the system's quality drop increases the network's robustness. Furthermore, shortening the total duration of the outage increases the rapidity of the recovery.

The many inherent uncertainties of the study (i.e., demand and production profiles, the timing and duration of the disaster, its impact, and the extent of subsequent phases, as well as fault detection times and restoration processes) call for a probabilistic approach [27]. To manage these uncertainty sources, this paper uses a Monte Carlo simulation. In particular, uncertainties related to load demand, distributed generation, and fault scenarios are modeled. This approach, by modeling each uncertain variable through stochastic sampling, allows for capturing the combined effect of multiple uncertain variables on system performance, providing a comprehensive representation of system behavior under different operating conditions. More specifically, a sufficiently large set of outage scenarios is constructed by sampling the status of each network component from a uniform distribution over [0, 1]. For each network element, if the sampled value is lower than the corresponding probability of failure under heatwave conditions, the element is considered to fail; otherwise, it remains operational. This procedure allows for the simultaneous failure of multiple components, thus extending beyond the traditional N–1 reliability framework to N–k contingency modeling.

As anticipated earlier, modeling the impact of heatwaves across all network elements remains a research challenge. Fragility curves are commonly used to relate the hazard intensity to the probability of failure of a given network component. For example, in [29–33], fragility curves for overhead lines and underground cables against windstorm and earthquake events are presented. Regarding heatwaves, developing an explicit and reliable model to estimate the probability of failure of exposed network components (e.g., MV cable joints) as a function of a heatwave indicator remains challenging. This correlation is inferred by the network operator [18] from recorded heatwave events and fault occurrences in such components, as described above. Generally, such information is not straightforward to obtain. To address this knowledge gap and maintain the methodology's general applicability, arbitrary failure probabilities are assigned to the selected network components in the simulations. The adopted failure probabilities are not intended to represent exact predictive models but rather to provide representative scenarios, given the current lack of robust, validated correlations between heatwave indicators and component failure probability. Then, by varying these probabilities within a reasonable range, a sensitivity analysis is performed to compare the effectiveness of different enhancement options as the probability of failure of network components increases.

The final stage involves evaluating the system response through power flow calculations over the time horizon of the extreme weather event. After the event, the fault location phase duration and the time required to organize repair crews are determined by sampling from a Weibull distribution. Furthermore, to capture the potential extension of the typical time to repair (TTR) under extreme conditions relative to normal operating scenarios, an additional temporal component is sampled from an exponential distribution. At this stage, the total recovery time is thus fully characterized.

The convergence criterion for stopping the sampling process is based on calculating the resilience area R_n at each nth extraction.

$$R_n = \int_{t_0}^{t_x} 100 \cdot [1 - X_n(t)] dt \tag{3}$$

$$\beta_n = \frac{\sqrt{\sigma(R_1, \cdots, R_n)}}{\mu(R_1, \cdots, R_n) \cdot \sqrt{n}} \leq \varepsilon \qquad n = 1 \ldots N \tag{4}$$

$$X_n(T) = \frac{P_S(t)}{P_D(t)} \tag{5}$$

where $X_n(t)$ is the system quality computed as the ratio between the power supplied in the disrupted conditions $P_S(t)$ and the total power demand $P_D(t)$ (i.e., the power that would have been supplied in non-disrupted conditions); t_0 and t_x are the initial and the final interval of the critical event (Figure 3); β_n is the convergence parameter; ε a given threshold; n is the number of the current extraction; and $\sigma(R_1, \cdots, R_n)$ and $\mu(R_1, \cdots, R_n)$ are, respectively, the variance and the mean value of the resilience area calculated until the n-th extraction. Once the convergence condition is met, the resilience metric is calculated as the mean ENS, which is proportional to the mean trapezoidal area $\mu(R_1, \cdots, R_N)$, where N is the number of outage scenarios analyzed to achieve convergence.

The high-level analysis index and the in-depth resilience assessment metrics characterize specific territorial areas, or entire networks, in aggregated form. This information can be used in a decision-support tool devoted to planning operational strategies and analyzing investment options. Operatively, as depicted in Figure 4, policymakers interested in identifying the most critical portions of a territory under investigation and properly orienting their investments toward a more resilient distribution system must divide the vast territory into smaller areas and collect the data reported in Table 1 (for this analysis). Most of the data, if not directly available, can be derived from open source databases. After normalizing the indicators and computing the risk index for each portion, they must select the areas that led to more critical outcomes in the first stage and, for the networks within those areas, apply the probabilistic resilience assessment, which constitutes the second stage of the methodology.

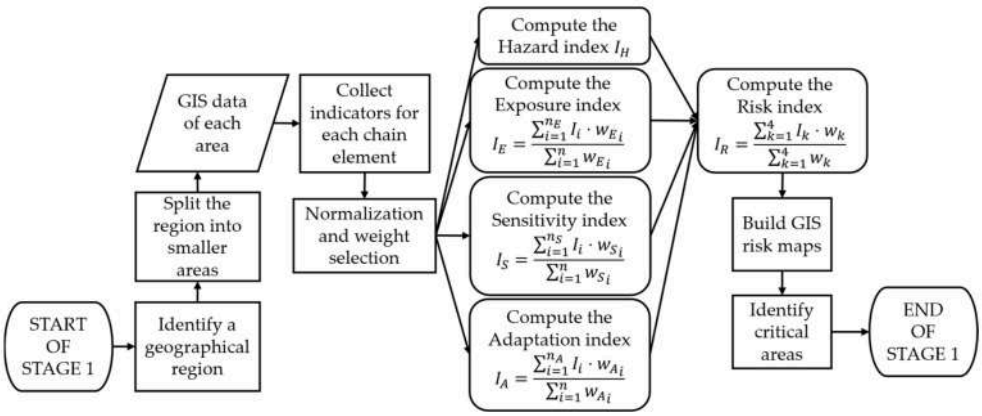

Figure 4. Workflow diagram of the first stage.

At this level, the number of selected areas depends on the subject's interests and on its computational and investment capabilities. The main advantage is that the analysis does not require investigating the entire distribution system (e.g., a national power distribution system) as in conventional approaches, but is focused only on the most critical portions, where investments need to be prioritized.

The diagram in Figure 5 depicts the main steps constituting the second stage of the methodology. Starting from the definition of component failure probabilities (e.g., for lines and joints under stress conditions), multiple contingency scenarios are generated. For each scenario, power-flow calculations are performed to evaluate network operability under N–k conditions.

The resulting system performance is then used to compute a time-dependent resilience metric (e.g., the ENS), typically based on the degradation and recovery of served load. This process is repeated across all simulated scenarios, enabling the estimation of expected resilience levels and the quantitative comparison of different network configurations or adaptation strategies.

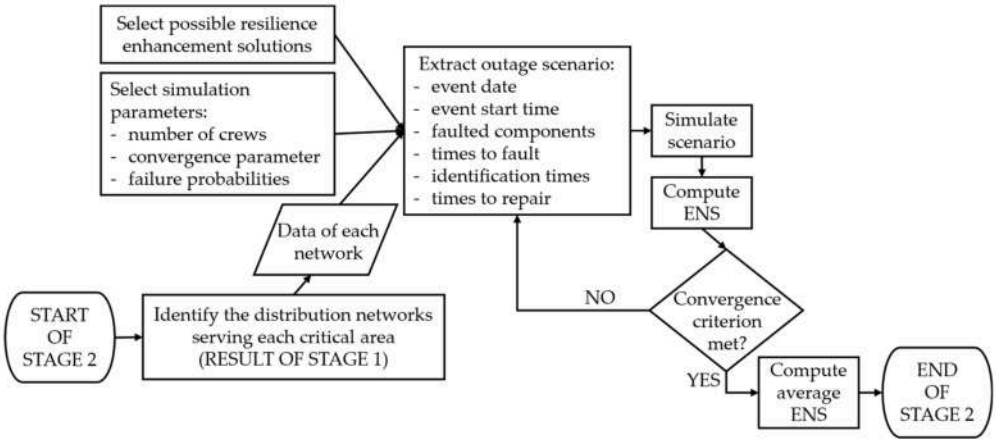

Figure 5. Workflow diagram of the second stage.

2.3. The Knowledge-Based Resilience Assessment Framework

Any process for assessing the climate-related resilience of power networks requires integrating climate and environmental data, network information, and numerical models [5]. Operational network analysis tools (e.g., power system simulators) have traditionally lacked capabilities for managing natural risk scenarios, while climate and environmental analysis tools, generally GIS-based, have developed separately. These two domains require different data types, management systems, analytical approaches, and expertise. To facilitate this interdisciplinary work, a flexible support technology can enable seamless integration of diverse data sources and analytical models, while ensuring adaptability to the specific needs of electricity infrastructure analysts and scalability to incorporate new data.

Knowledge graph technology has been developed within the NEST project, specifically to support the resilience analysis of an electricity network [16]. Knowledge graphs represent data from different interconnected domains under a unified semantic layer. Unlike conventional relational databases, the semantic representation of entities and relationships enables the integration of heterogeneous data sources despite differences in their underlying schemas. This semantic layer consists of an ontology that can be queried using standard logic-based languages and is utilized to build automated reasoning rules. The developed ontology, named the Ontology for Systemic Analysis of Resilient Electricity Networks, has a modular structure and can represent interconnections with environmental, socio-economic, and engineering systems that may influence the operation of the electricity infrastructure. The semantic model can be extended to map data and computational models, which can be associated with services, either by specifying endpoints or by simply describing their characteristics. A key advantage of this technology is its ability to adapt to specific application requirements and to be deployed as a SPARQL endpoint.

A sketch of the semantic model defined for this work is presented in Figure 6. The ontology models the relationship between climatic hazard conditions and their impact on power network resilience. At its core, *Climatic Influence* is an abstract class that represents a climatic condition derived from a *Heatwave Indicator* affecting a *Geographic Area*. A Geographic Area can be hierarchically decomposed into sub-areas, each associated with a specific value of the *Heatwave Indicator*.

The assessment of climatic influence is described in a *Hazard GIS Model*, a geospatial dataset (e.g., a geopackage) containing the spatiotemporal distribution of hazard values. In this implementation, the spatially dense hazard results (i.e., raster-cell-level indicator values) are stored within the GIS package. At the same time, the knowledge graph serves as a lightweight semantic integration layer linking infrastructure assets, geographic partitions,

and analysis artifacts to the corresponding GIS layers. This dataset serves as the input to a *Resilience Assessment Method*, which computes the *Operational Resilience* results and outputs them as a *Resilience GIS Model*. Both GIS models represent structured, geospatially referenced information that can be visualized in a GIS environment.

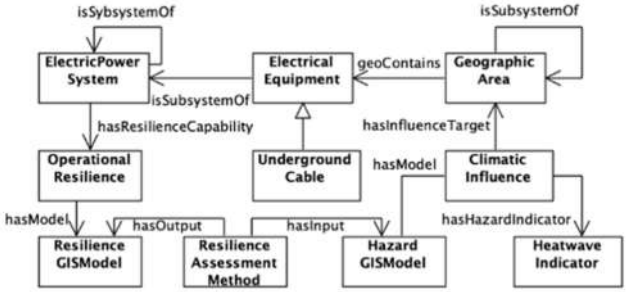

Figure 6. UML diagram of the semantic model fragment linking climate analysis for heatwave detection to the operational resilience assessment based on the characteristics of exposed underground cables.

The knowledge graph is populated through support tools that acquire both climatic data from external open repositories, such as the Euro-Mediterranean Center on Climate Change (CMCC) Data Delivery System (DS) [34], and geolocalized network data to be analyzed. These codes must be specifically implemented for the intended application.

3. Results

This section presents the setup of a test-bed analysis environment that leverages open climatic data and applies the resilience assessment methodology to a representative network case study, thereby demonstrating the approach's effectiveness.

3.1. Context Description

The first step is to identify the network model to be analyzed within a specific geographic area of interest. To this aim, a representative portion of the distribution system, typical of the Italian urban context and derived from the ATLANTIDE project [35], has been placed within a pre-defined urban area in Rome. In that project, urban networks were identified using a set of socio-economic and electrical indicators (e.g., population density, electricity consumption, and RES penetration), ensuring their representativeness of real operating conditions. In addition, the ATLANTIDE project supported the definition of evolutionary scenarios of distribution system development, accounting for the combined evolution of load demand, distributed generation, renewable energy penetration, and emerging technologies such as electric vehicles. These scenarios are derived from macroeconomic and policy-driven assumptions and are used to represent plausible future operating conditions of the network. In particular, both baseline (business-as-usual) and more advanced transition scenarios were considered, enabling the assessment of network performance as electrification and RES integration increase. The representative urban network used in this paper is characterized by high-density loads, a large number of LV customers supplied by many MV/LV substations, and short underground cable lines (the maximum line length is about 4 km). The urban network consists of a primary substation with a 40 MVA HV/MV transformer that feeds 96 MV nodes, divided into 11 feeders. Figure 7 shows a schematic representation of the test urban network. The total nominal load demand, split between residential, commercial, office, and small industrial customers, is about 26 MVA at the peak of the starting year (about 40 MVA in 2030). Although the generation (i.e., photovoltaics) in the urban context is generally connected to the LV level, the

installed power (i.e., about 110 MW at 2030 in the business-as-usual scenario) is aggregated to the MV side of the relevant MV/LV node.

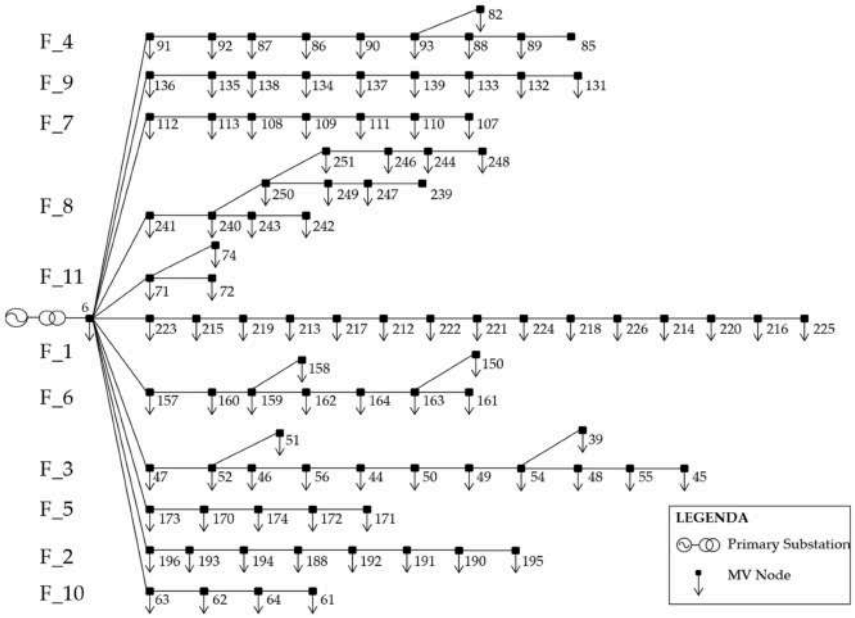

Figure 7. Scheme of the representative urban distribution network used as a case study.

To assess and plan the network's resilience under future climate scenarios, high-resolution projections, specifically the RCP 4.5 and RCP 8.5 scenarios developed by CMCC at ~2.2 km resolution over Italy, have been employed [36]. The datasets, available via API and providing time series of hourly temperature and precipitation for every year up to 2100, have been reduced for illustrative purposes to the target years 2030, 2050, and 2070 due to their large size. In line with ARERA's guidelines, the analysis considers the months from May to September. Using different climate scenarios explicitly incorporates uncertainty in future conditions into the analysis while demonstrating the robustness of the proposed framework.

3.2. Hazard Model

The climate data acquisition and processing are supported by a Python 3.10 script that, given the geolocated network, identifies the relevant portion of the climate grid to be retrieved from the CMCC DS, projects it over the network area, and associates each cell with the corresponding hazard indicator, as defined by ARERA, within the selected temporal window. This process is illustrated in Figure 8.

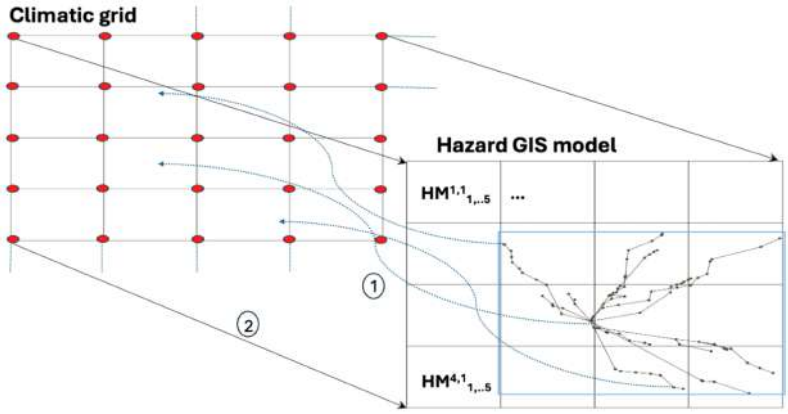

Figure 8. Climatic data acquisition and generation of the hazard GIS model.

To ensure full network coverage, the bounding box of the geographic area must be aligned with multiples of the CMCC grid spacing. This guarantees that all cells containing the objects of interest (the network nodes, in this case) are detected.

Optionally, a one-cell buffer is added around the network, not strictly for coverage, but to account for potential topology changes or extensions, which could help test improvements in resilience. It is noted that for CMCC downscaled datasets, the grid is rotated, and the cell angles are only approximately 90° when mapped. However, the dataset provides the coordinates of the grid nodes as 2D lat/lon, and the time series of the air temperature and precipitation variables are associated with these nodes. Furthermore, cells defined by lat/lon are not perfectly square, as the length of a degree of longitude changes with latitude.

For each node of the climate grid, the daily heatwave index is computed for each year and month using the ARERA HWI formula described in Section 2.1.

Figure 9 shows the index series for two opposite nodes of the network's coverage grid. A higher frequency of index values above the threshold can be observed in 2050 compared to 2030, with slight differences between the two nodes. Then, the monthly index HMi (i = 1, . . ., 5) is obtained by summing the HTW values that exceed 10 over all days of the month. The cell is assigned the average values of its four corner nodes.

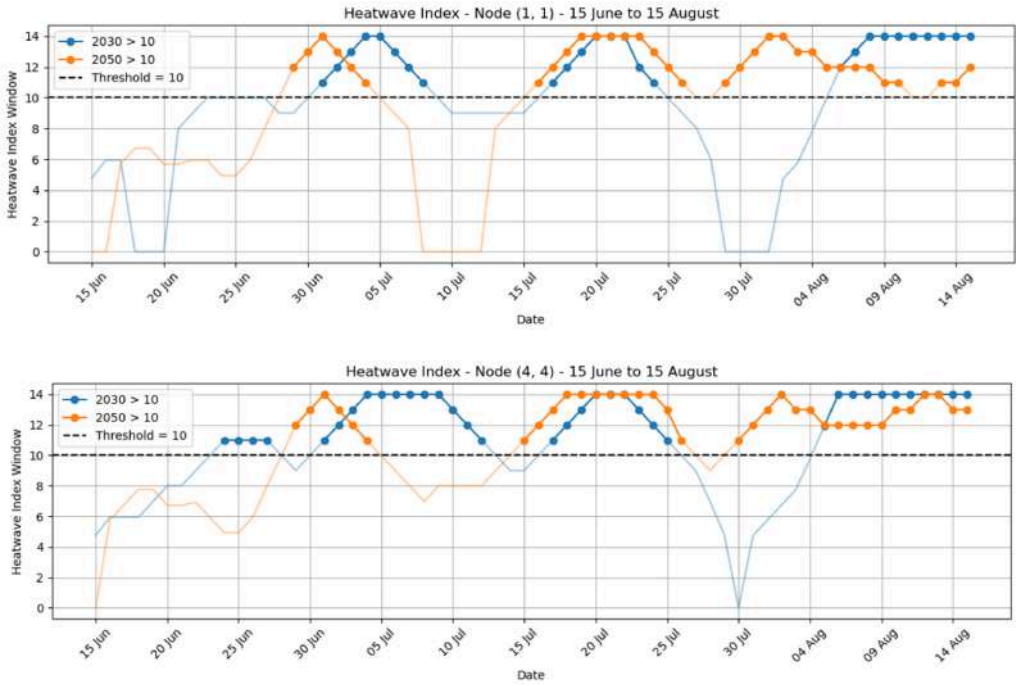

Figure 9. Series of the ARERA heatwave index calculated over 7-day sliding windows, from 15 June to 15 August, under the RCP4.5 climate scenario.

All the results, including the geographic area, monthly heatwave indicator values, and geometries, are stored in a geo-package (i.e., the Hazard GISModel) to support subsequent analyses within the resilience assessment method described in Section 2.3.

3.3. Resilience Assessment Results

Many different versions of the procedure were implemented to highlight its capabilities, including variations in the RCP scenario, the selected target year, the weighting of impact chain components, and the application of a mitigation measure, to assess the procedure's effectiveness in visualizing improvements from resilience-oriented planning interventions. A sample of the preliminary screening results from applying the impact chain approach to the test network is presented in Figure 9, which compares the three most representative months across two target years (i.e., 2030 and 2050) under the RCP 4.5 scenario.

In particular, the results of Figure 10 are achieved by averaging with suitable weights (in accordance with (2)), the hazard (calculated as in (1)), the exposure, sensitivity, and adaptation indicators listed in Table 1, for each square on which the portion of territory is subdivided. Table 2 reports the values of these indicators (i.e., for the entire test network) with the weights used in the calculation.

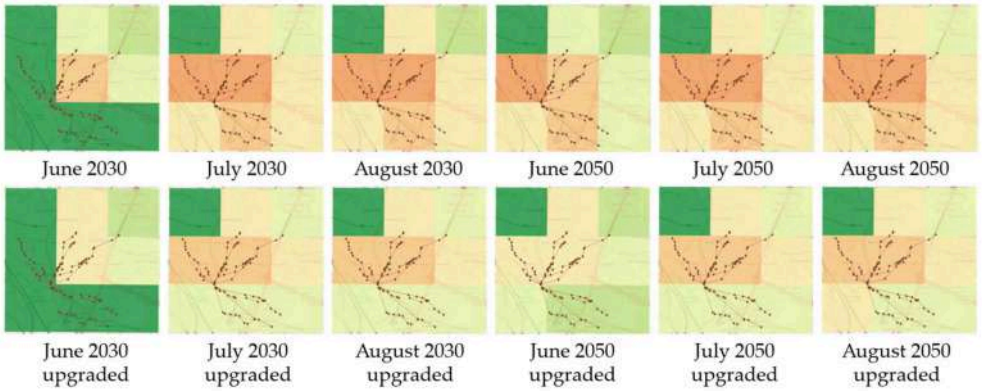

Figure 10. Results of the first screening.

Table 2. Values of the indicators and relevant weights used in the case study.

	Indicator	Weight	Value
Hazard	Heatwaves index $I_{heatwave}$ (as defined in (1))	1	0 (min)–374 (max)
Exposure	Underground cable length	0.2	27.82 km
	Number of joints	0.7	273
	Joint average age	0.1	10
Sensitivity	Number of LV customers	0.1	45,423
	Number of MV customers	0.15	49
	Number of prosumers	0.2	70
	Number of premium customers	0.55	62
Adaptation	Distributed generation or storage installed power	0.7	111 MW
	Trunk nodes	0.3	78

The selection of weighting factors can significantly influence indicator aggregation. A detailed assessment of weighting strategies and their effectiveness in supporting the validation of the methodology is presented in [27]. In this study, the numerical values of the weights are provided as a representative example to illustrate the application of the proposed framework. The methodology itself is not dependent on a specific set of weights and remains valid under different weighting configurations. Furthermore, the framework is designed to accommodate subjective contributions from decision-makers, enabling the definition of context-specific weights based on priorities, planning objectives, and targeted investment strategies. This flexibility enhances the approach's practical applicability in real-world decision-making processes. This feature enables tailoring the analysis to different policy perspectives without altering the underlying methodological structure.

According to the chromatic scale in Figure 11, the results are compared between the base case and an "upgraded" configuration. The base case represents the existing network, while the upgraded scenario incorporates a resilience-enhancing measure proposed by the main Italian DSO to increase network robustness [37]. Specifically, as the most straightforward approach to mitigating the heatwave phenomenon is to reduce the number of

joints during construction, the proposed solution is to use single-pole cables instead of triplex cables, thereby increasing the available branch length. It is important to note that in urban areas, multiple angles and physical interferences are common; hence, innovative and alternative installation techniques and tools must be explored to facilitate joint reduction. Accordingly, the decrease in the number of joints has been explicitly evaluated in the proposed case study, and the upgraded case shows a reduction of almost 30%.

Value	Color	Criticality level
0.0 – 0.1		Low
0.1 – 0.2		
0.2 – 0.3		Low to medium
0.3 – 0.4		
0.4 – 0.5		Medium
0.5 – 0.6		
0.6 – 07		Medium to high
0.7 – 0.8		
0.8 – 0.9		High
0.9 – 1.0		

Figure 11. Chromatic scale of the results.

Once a portion of the network is identified as critical on the maps, the second step of the procedure characterizes the network using the proposed metric and assesses its resilience in detail. The resilience metric adopted is the mean ENS, calculated both for the base case and, for demonstrating the effectiveness of the methodology, after implementing three improvement measures: (i) the reduction in the number of MV cable joints, (ii) the subdivision of the grid into LV microgrids, defined as those involving only a single MV/LV node, and (iii) the subdivision into MV microgrids, defined as those encompassing more than one MV/LV node. The first option can be classified as an infrastructure resilience enhancement that increases the grid's robustness. In contrast, the second and third options are operational alternatives that involve implementing an operational strategy based on a defined plan in advance and are considered the most promising resilience enhancement solutions [38,39].

Given the lack of an explicit correlation between the hazard indicator adopted in this study and the probability of failure of the vulnerable network components, the probabilistic analysis is conducted by assuming a hazard intensity that increases the failure probability of the joints from 10% to 50%. Furthermore, the speed of the restoration phase depends solely on the number of available crews at the time of the extreme event. In modeling this phase, it is assumed that a sufficient number of maintenance crews are available to repair faults as they occur. The impact of repair crew availability on system performance was systematically analyzed in [29]. Beyond a certain threshold, no significant improvement in restoration performance is observed. Therefore, the number of available crews adopted in this paper (i.e., eight crews) reflects a trade-off between resource allocation and operational effectiveness.

Finally, without affecting generality, the convergence threshold is set to 0.01, leading, on average, to about 1000 Monte Carlo iterations per simulation. This choice ensures that a sufficiently large number of outage scenarios are analyzed, so that the final results can be considered statistically significant.

Table 3 and Figure 12 present the main results of the study: the average trapezoidal area computed across multiple simulated scenarios of failure probability.

Table 3. Results: resilience performance.

		Resilience Metric [MWh]				
Case	Base	122.97	244.21	347.69	436.84	512.23
	Reduced number of joints	78.35 (−36.3%)	159.74 (−34.6%)	235.53 (−32.3%)	308.4 (−29.4%)	372.97 (−27.2%)
	LV microgrids	85.68 (−30.3%)	164.55 (−32.6%)	231.29 (−33.5%)	287.49 (−34.2%)	334.99 (−34.6%)
	MV microgrids	57.99 (−52.8%)	109.93 (−55.0%)	155.21 (−55.4%)	192.93 (−55.8%)	224.59 (−56.2%)
Failure probability		0.1	0.2	0.3	0.4	0.5

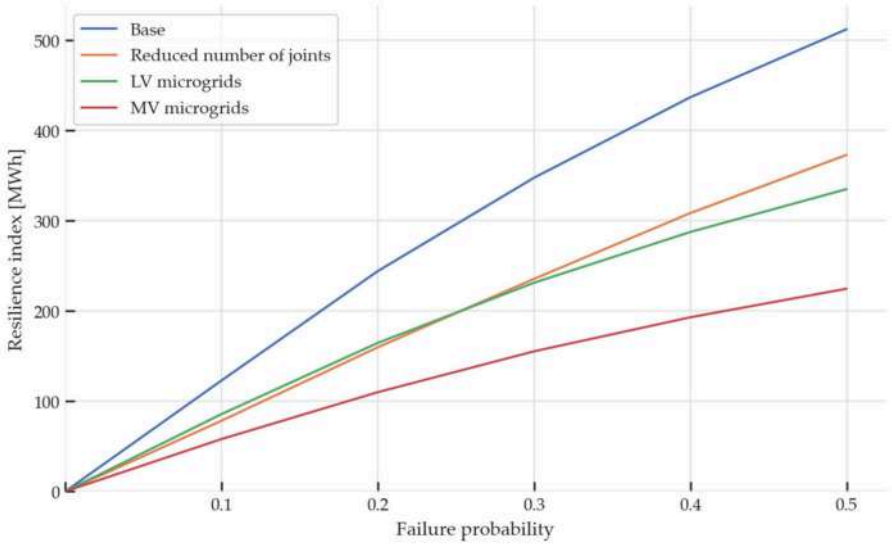

Figure 12. Results: resilience performance obtained by varying the failure probability of the joints.

4. Discussion

The first step of the resilience assessment procedure provides a spatial representation of the hazard indicator under the RCP 4.5 scenario for three representative summer months (June, July, and August) in two target years (2030 and 2050). Figure 10 compares the base case configuration, representative of the existing network, with the upgraded configuration in which single-pole cables replace triplex cables, thereby reducing the number of joints and increasing the available branch length. Figure 11 shows the chromatic scale used in the results.

In the base case (top row of Figure 10), the maps for July and August, particularly in 2050, show a predominance of medium-to-high-risk areas (yellow to orange tones), indicating increased exposure and vulnerability of the network to heatwave conditions. June generally exhibits lower risk levels, although a progressive deterioration is observed toward 2050. The upgraded configuration (bottom row of Figure 10), i.e., the adoption of single-pole cables instead of triplex cables, reduces the number of joints, increasing branch lengths and reducing the exposure index, exhibits a visible reduction in the extent of medium/high-risk areas, with a shift toward lower risk classes (greener tones) across all months. The risk index reduction is evident, especially in June 2030 and June 2050, but there are also noticeable improvements in high-risk months such as July and August. The spatial reduction of the orange/red areas confirms that the mitigation measure lowers the overall risk index across the network. The maps clearly highlight the combined effect of climate change (risk intensification toward 2050) and the mitigating potential of targeted design measures in reducing component vulnerability.

The results of the first stage inherently guide the second stage of the methodology. In large-scale real-world applications, the first stage serves as a filtering mechanism, enabling the identification of the most critical portions of the distribution network that require a more detailed resilience assessment. In the case study presented in this work, the system's geographical extent is limited; therefore, it was not necessary to restrict the second-stage analysis to specific network segments. For larger systems, it is recommended to adopt a spatial resolution that enables the second stage to be applied to individual distribution networks supplied by primary substations, thereby ensuring computational tractability while preserving analysis accuracy.

The second step of the procedure evaluates network resilience using the trapezoid area as a quantitative metric. From Table 3 and Figure 12, it can be observed that the base case, which represents the benchmark system performance, yields an average resilience area ranging from 122.97 MWh to 512.23 MWh, depending on the assumed joint failure probability (i.e., from 10% to 50%). Obviously, the higher the failure probability, the worse the metric. The infrastructure resilience option, i.e., reducing the number of joints, produces significant improvements, reducing the metric from a maximum of about 36% (i.e., 78.35 MWh vs 122.97 MWh) to a minimum of about 27% (i.e., 372.97 MWh vs 512.23 MWh).

The LV microgrid arrangement reduces the resilience area by about one-third for the smallest joint failure probability (i.e., −30.3% with 10% failure probability), indicating faster recovery and/or reduced service disruption, but proving to be less effective than the infrastructure option in the same case. However, as the failure probability increases, resorting to such an operational option becomes more effective than reducing the number of joints (e.g., −34.6% with 50% of failure probability). Creating MV microgrids achieves the largest improvement, with an over 50% reduction in the resilience area, by enabling intentional islanding across larger network portions, thereby increasing the system's robustness and adaptability under stress.

It is important to note that, in the current implementation, DERs are modeled using time-dependent generation profiles that vary by time, day, month, and year of the simulation. These profiles implicitly capture seasonal effects, including the typical reduction in photovoltaic (PV) efficiency due to higher temperatures. However, no additional derating of PV generation or explicit modeling of battery performance degradation is introduced under extreme heatwave conditions. The inclusion of temperature-dependent performance models for DERs, such as PV efficiency degradation at extreme temperatures or battery capacity constraints, extends the proposed framework and is identified as a direction for future work.

Overall, the results demonstrate the complementarity between the two stages of the proposed approach. The first stage, through the risk mapping, supports the identification of vulnerable areas and the appraisal of targeted mitigation measures. The second stage quantifies the performance gains achievable through advanced operational strategies, thereby providing planners with a comprehensive basis for selecting effective resilience-oriented interventions.

Although MV microgrids appear to be the most effective solution, these results do not account for implementation costs. Regarding investment costs, reducing the number of joints on an existing cable line is effectively equivalent to constructing a new line. This is because excavation works, the purchase of new conductors and joints, and the additional dismantling of the existing line must all be accounted for. Therefore, the greater the number of kilometers of lines to be substituted, the higher the cost of this improvement solution. On the other hand, implementing LV and MV microgrids involves significant investments due to the cost of additional remote-controlled switches for automatic network reconfiguration.

Such additional switches can be more numerous in the MV microgrid solution, because, hypothetically, all MV network nodes need to be separated.

In contrast, in the LV microgrid solution, only nodes with generation may need to be disconnected from the rest of the network. Furthermore, the purchase of energy storage systems should be considered as additional CAPEX. The size and cost of these energy storage systems can be considered proportional to the hourly difference between PV production and each microgrid's demand, and thus statistically calculated across the simulated scenarios. Nevertheless, such operational solutions (i.e., the MV and LV microgrids) are self-reliant and can be adopted even in the event of transmission system failure. For these and many other relevant reasons, it is strongly suggested that a trade-off be found between resilience benefits and investment.

5. Conclusions

This paper presents selected results from the activities of Spoke 8, WP 8.5 "Climate change adaptation and energy system" of the project "Network 4 Energy Sustainable Transition—NEST", funded under the National Recovery and Resilience Plan (NRRP).

The paper focuses on the resilience of power distribution systems to one of the most critical extreme events expected due to climate change: heatwaves. A preliminary description of the framework was presented in [17], which this paper extends.

The first part of the paper discusses the hazard, i.e., the heatwave event, and its characterization in terms of the failure risk of the affected network components. It then details a two-stage method that first identifies the portions of power distribution systems most critical with respect to the given hazard and then investigates them in greater depth by assessing suitable resilience metrics. Furthermore, the paper describes how all relevant information for resilience analysis can be integrated into a tool based on knowledge graph technology. Compared to other works, this approach provides greater technological flexibility by enabling the use of different resilience models within the same framework. Applied to a representative case study, the framework demonstrates the effectiveness of the proposed approach in automating significant use cases, enabling integration with optimization tools to assist operators in formulating operational planning strategies and selecting appropriate investments.

Given the acknowledged lack of robust, universally accepted models linking heatwave indicators to component failure probability, the failure probabilities adopted in this study should be interpreted as representative scenarios rather than exact predictive values. To address this limitation and assess the robustness of the results, a sensitivity analysis has been conducted by varying the assumed failure probability over a wide range. This allows us to evaluate the extent to which the main findings depend on the adopted assumptions. The results of this analysis show that, although the absolute values of system performance metrics vary with the assumed failure probability, the relative trends and the comparative effectiveness of the proposed strategies remain consistent. Therefore, the conclusions of this study are not significantly affected by the absence of a direct correlation between climate indicators and failure probability. This approach enables us to overcome the current lack of explicit correlation models while still providing meaningful insights into system behavior under stress conditions.

The validation of the proposed resilience metrics against real outage data or historical extreme-heat events is currently limited by the lack of publicly available, high-resolution datasets that simultaneously include detailed network information, climatic conditions, and failure records. In this context, the objective of the present work is primarily methodological, aiming to provide a structured framework for resilience assessment rather than a direct predictive tool calibrated on specific real-world datasets. The proposed approach is

designed to be applied by system operators and policymakers, who have access to detailed, proprietary data, enabling more accurate calibration and validation of the methodology in real operational contexts. Therefore, while a direct validation is not feasible within this study, the framework provides a consistent and adaptable basis for supporting decision-making when appropriate data are available. This reflects a common limitation in resilience studies under extreme events, where data scarcity constrains direct empirical validation.

However, future works should focus on validating the proposed framework against historical outage datasets and calibrating the failure models using observed utility records to strengthen the methodology's predictive reliability and operational applicability. In addition, the framework should be extended to account for multiple heat-sensitive component classes, such as transformers and protection devices, to evaluate how marked multi-component failure mechanisms may affect the resulting risk maps and resilience rankings.

Furthermore, since a comprehensive cost–benefit comparison between microgrid deployment and traditional infrastructure upgrades is not included in this work, future work will integrate economic evaluation metrics to complement the methodological approach presented here, enabling a more comprehensive assessment of alternative investment strategies. This aspect represents a significant extension of the proposed framework and is currently under investigation as part of ongoing research. This extension will allow for bridging the gap between technical assessment and investment decision-making.

Author Contributions: Conceptualization, L.C., F.P., G.P., M.P. (Massimo Pompili) and M.L.V.; Methodology, A.C., G.P., M.P. (Maurizio Pollino) and M.L.V.; Software, A.C., and M.L.V.; Validation, A.C. and G.P.; Formal analysis, A.C. and G.P.; Resources, M.P. (Maurizio Pollino), M.P. (Massimo Pompili) and M.L.V.; Data curation, M.P. (Maurizio Pollino) and M.L.V.; Writing—original draft, L.C., A.C., G.P. and M.L.V.; Writing—review & editing, L.C., A.C., F.P., G.P., M.P. (Massimo Pompili) and M.L.V.; Visualization, A.C. and M.L.V.; Supervision, F.P., G.P. and M.P. (Massimo Pompili); Project administration, F.P. and M.P. (Massimo Pompili); Funding acquisition, F.P. and M.P. (Massimo Pompili). All authors have read and agreed to the published version of the manuscript.

Funding: This work has been developed within the project funded under the National Recovery and Resilience Plan (NRRP), Mission 4 Component 2 Investment 1.3—Call for tender No. 341 of 15.03.2022 of Ministero dell'Università e della Ricerca (MUR); funded by the European Union—NextGenerationEU. Award Number: Project Code code PE0000021, Concession Decree No. 1561 of 11.10.2022 adopted by Ministero dell'Università e della Ricerca (MUR), CUP F53C22000770007, Project title "Network 4 Energy Sustainable Transition—NEST".

Data Availability Statement: The original contributions presented in this study are included in the article. Further inquiries can be directed to the corresponding author.

Conflicts of Interest: The authors declare no conflict of interest.

References

1. IEA. *Climate Resilience for Energy Security*; IEA: Paris, France, 2022. Available online: https://www.iea.org/reports/climate-resilience-for-energy-security (accessed on 15 April 2026).
2. IEA. *World Energy Outlook 2025*; IEA: Paris, France, 2025. Available online: https://www.iea.org/reports/world-energy-outlook-2025 (accessed on 15 April 2026).
3. Gentilini, I.; Baresi, L.; Citin, L.B.; Biloslavo, A.; Dall'Acqua, D.; Dalla Costa, G.; Di Felice, G.; Ferrante, M.; Forciniti, S.; Leggio, A.; et al. Data driven analysis of underground MV joint failure phenomena in the Italian distribution grid. In Proceedings of the CIRED 2025 Conference, no. 1237, Geneva, Switzerland, 16–19 June 2025. [CrossRef]
4. FEMA. HAZUS-MH Platform. Available online: https://www.fema.gov/flood-maps/products-tools/hazus (accessed on 11 August 2025).
5. Villani, M.L.; Giovinazzi, S.; Pollino, M.; Corsini, A. Resilience Analysis of Electricity Networks to Compound Hazards Using GIS and Semantic Tools. *IEEE Trans. Ind. Appl.* **2026**. [CrossRef]

6. Ciapessoni, E.; Cirio, D.; Pitto, A. An Efficient Methodology to Identify Relevant Multiple Contingencies and Their Probability for Long-Term Resilience Studies. *Energies* **2024**, *17*, 2028. [CrossRef]
7. Ciapessoni, E.; Cirio, D.; Pitto, A.; Carlini, E.M.; Marzullo, F.; Casulli, S.; Lazzarini, A.; Falorni, F.; Scavo, F.; Berrettoni, G.; et al. An innovative methodology for risk-based resilience assessment to prioritize grid interventions against natural threats in the Italian power system. *Environ. Syst. Decis.* **2026**, *46*, 4. [CrossRef]
8. Paul, S.; Poudyal, A.; Poudel, S.; Dubey, A.; Wang, Z. Resilience assessment and planning in power distribution systems: Past and future considerations. *Renew. Sustain. Energy Rev. Part B* **2024**, *189*, 113991. [CrossRef]
9. Montalà-Palau, M.; Cheah Mañé, M.; Gomis-Bellmunt, O. How resilient is a power system? An open-source tool integrating GIS and Optimal Power Flow for resilience assessment. *Energy Nexus* **2026**, *21*, 100630. [CrossRef]
10. Montalà-Palau, M.; Cheah Mañé, M.; Gomis-Bellmunt, O. GIS-based approach to improve the resilience of the distribution network. In Proceedings of the CIRED Chicago Workshop 2024: Resilience of Electric Distribution Systems, Chicago, IL, USA, 7–8 November 2025; pp. 138–142. [CrossRef]
11. Campos, R.; Harvey, P.S., Jr.; Kays, H.M.I.; Panchalogaranjan, V.; Moses, P.S.; Sadri, A.M. Resilience assessment of electrical distribution networks subject to wind and self-induced fire hazards. *Reliab. Eng. Syst. Saf.* **2026**, *274*, 112411. [CrossRef]
12. Zebisch, M.; Terzi, S.; Pittore, M.; Renner, K.; Schneiderbauer, S. Climate Impact Chains—A Conceptual Modelling Approach for Climate Risk Assessment in the Context of Adaptation Planning. In *Climate Adaptation Modelling*; Springer Climate: Cham, Switzerland, 2022.
13. Intergovernmental Panel on Climate Change. *Climate Change 2014: Impacts, Adaptation, and Vulnerability*; Contribution of Working Group II to the Fifth Assessment Report of the Intergovernmental Panel on Climate Change; Field, C.B., Barros, V.R., Dokken, D.J., Mach, K.J., Mastrandrea, M.D., Bilir, T.E., Chatterjee, M., Ebi, K.L., Estrada, Y.O., Genova, R.C., et al., Eds.; Cambridge University Press: Cambridge, UK, 2014. Available online: https://www.ipcc.ch/report/ar5/wg2/ (accessed on 15 April 2026).
14. Atrigna, M.; Buonanno, A.; Carli, R.; Cavone, G.; Scarabaggio, P.; Valenti, M.; Graditi, G.; Dotoli, M. A Machine Learning Approach to Fault Prediction of Power Distribution Grids Under Heatwaves. *IEEE Trans. Ind. Appl.* **2023**, *59*, 4835–4845. [CrossRef]
15. Leite, J.B.; Mantovani, J.R.S.; Dokic, T.; Yan, Q.; Chen, P.-C.; Kezunovic, M. Resiliency Assessment in Distribution Networks Using GIS-Based Predictive Risk Analytics. *IEEE Trans. Power Syst.* **2019**, *34*, 4249–4257. [CrossRef]
16. Villani, M.L. ENEA Infraresilience KG. 2025. Available online: https://gitlab.com/nest854/enea-ics-infraresilience-kg (accessed on 15 April 2026).
17. Calcara, L.; Casu, A.; Pilo, F.; Pisano, G.; Pollino, M.; Pompili, M.; Villani, M.L. Mapping Resilience of Distribution Networks Against Heatwaves. In Proceedings of the 2024 AEIT International Annual Conference (AEIT), Trento, Italy, 25–27 September 2024; pp. 1–6. [CrossRef]
18. Calcara, L.; D'Orazio, L.; Della Corte, M.; Di Filippo, G.; Pastore, A.; Ricci, D.; Pompili, M. Faults Evaluation of MV Underground Cable Joints. In Proceedings of the AEIT International Annual Conference, Florence, Italy, 18–20 September 2019. [CrossRef]
19. Pompili, M.; Calcara, L.; D'Orazio, L.; Ricci, D.; Derviskadic, A.; He, H. Joints defectiveness of MV underground cable and the effects on the distribution system. *Electr. Power Syst. Res.* **2021**, *192*, 107004. [CrossRef]
20. ARERA—Autorità di Regolazione per Energia Reti e Ambiente. *Annual Report—Summary 2023*; ARERA: Milan, Italy, 2023.
21. Afzal, S.; Mokhlis, H.; Illias, H.A.; Mansor, N.N.; Shareef, H. State-of-the-art review on power system resilience and assessment techniques. *IET Gener. Transm. Distrib.* **2021**, *14*, 6107–6121. [CrossRef]
22. Yao, Y.; Liu, W.; Jain, R. Power System Resilience Evaluation Framework and Metric Review. In Proceedings of the 2022 IEEE Power & Energy Society Innovative Smart Grid Technologies Conference (ISGT), New Orleans, LA, USA, 24–28 April 2022; pp. 1–5. [CrossRef]
23. Das, L.; Munikoti, S.; Natarajan, B.; Srinivasan, B. Measuring smart grid resilience: Methods, challenges and opportunities. *Renew. Sustain. Energy Rev.* **2020**, *130*, 109918. [CrossRef]
24. Vugrin, E.D.; Castillo, A.R.; Silva-Monroy, C.A. *Resilience Metrics for the Electric Power System: A Performance-Based Approach*; Sandia National Laboratories: Albuquerque, NM, USA, 2017. [CrossRef]
25. Yuan, W.; Wang, J.; Qiu, F.; Chen, C.; Kang, C.; Zeng, B. Robust Optimization-Based Resilient Distribution Network Planning Against Natural Disasters. *IEEE Trans. Smart Grid* **2016**, *7*, 2817–2826. [CrossRef]
26. European Distribution System Operators (EDSO). Position Paper Climate Resilience Metrics for Electricity Grids. Available online: https://www.edsoforsmartgrids.eu/content/uploads/2024/06/e.dso-position-paper-climate-resilience-metrics-for-electricity-grids.pdf (accessed on 11 August 2025).
27. Casu, A.; Pilo, F.; Pisano, G.; Soma, G.G. Operational Planning Strategies for Improving the Resilience of Electricity Distribution Systems Supplying Critical Loads. In Proceedings of the 2024 IEEE International Humanitarian Technologies Conference (IHTC), Bari, Italy, 25–27 November 2024; pp. 1–6. [CrossRef]

28. De Masi, M.; Valtorta, G.; Amicarelli, E.; Suich, A.; Danesin, A.; Dura, F.; De Berardinis, E.; Marcelli, A. Resilience Enhancement of MV Distribution Grids Against Snowstorms. In Proceedings of the CIRED 2019, no. 1618, Madrid, Spain, 3–6 June 2019. [CrossRef]
29. Casu, A.; Pilo, F.; Pisano, G.; Soma, G.G. Operational strategy modeling for enhancing distribution network resilience assessment. In Proceedings of the 2025 IEEE International Conference on Environment and Electrical Engineering (EEEIC/I&CPS Europe), Chania, Greece, 15–18 July 2025.
30. Panteli, M.; Mancarella, P.; Trakas, D.N.; Kyriakides, E.; Hatziargyriou, N.D. Metrics and Quantification of Operational and Infrastructure Resilience in Power Systems. *IEEE Trans. Power Syst.* **2017**, *32*, 4732–4742. [CrossRef]
31. Panteli, M.; Mancarella, P. Modeling and Evaluating the Resilience of Critical Electrical Power Infrastructure to Extreme Weather Events. *IEEE Syst. J.* **2017**, *11*, 1733–1742. [CrossRef]
32. Espinoza, S.; Poulos, A.; Rudnick, H.; de la Llera, J.C.; Panteli, M.; Mancarella, P. Risk and Resilience Assessment with Component Criticality Ranking of Electric Power Systems Subject to Earthquakes. *IEEE Syst. J.* **2020**, *14*, 2837–2848. [CrossRef]
33. Shaeezadeh, A.; Onyewuchi, U.P.; Begovic, M.M.; DesRoches, R. Age-Dependent Fragility Models of Utility Wood Poles in Power Distribution Networks Against Extreme Wind Hazards. *IEEE Trans. Power Deliv.* **2013**, *29*, 131–139. [CrossRef]
34. Euro-Mediterranean Center on Climate Change (CMCC). Data Delivery System (DS). Available online: https://dds.cmcc.it/ (accessed on 15 April 2026).
35. Bracale, A.; Caldon, R.; Celli, G.; Coppo, M.; Dal Canto, D.; Langella, R.; Petretto, G.; Pilo, F.; Pisano, G.; Proto, G.; et al. Analysis of the Italian distribution system evolution through reference networks. In Proceedings of the IEEE PES ISGT Europe, Berlin, Germany, 14–17 October 2012.
36. Raffa, M.; Adinolfi, M.; Reder, A.; Marras, G.F.; Mancini, M.; Spicione, G.; Santini, M.; Mercogliano, P. Very High Resolution Projections over Italy under different CMIP5 IPCC scenarios. *Sci. Data* **2023**, *10*, 238. [CrossRef] [PubMed]
37. Gentilini, I.; Bartolucci, M.; Calone, R.; Chiarenza, A.; Dall'Acqua, D.; D'Orazio, L.; Di Felice, G.; Dura, F.; Esteban Santamaria, M.C.; Grecchi, L.; et al. New Design Criteria for MV Underground Feeders to Enhance Network Resilience in the Energy Transition and Climate Change Era. In Proceedings of the CIRED 2025 Conference, no. 1172, Geneva, Switzerland, 16–19 June 2025. [CrossRef]
38. Wang, Y.; Qiu, D.; Teng, F.; Strbac, G. Towards Microgrid Resilience Enhancement via Mobile Power Sources and Repair Crews: A Multi-Agent Reinforcement Learning Approach. *IEEE Trans. Power Syst.* **2024**, *39*, 1329–1345. [CrossRef]
39. Qiu, D.; Strbac, G.; Wang, Y.; Ye, Y.; Wang, J.; Pinson, P.; Silva, V.; Teng, F. Artificial Intelligence for Microgrid Resilience: A Data-Driven and Model-Free Approach. *IEEE Power Energy Mag.* **2024**, *22*, 18–27. [CrossRef]